

Application of confocal laser microscopy for monitoring mesh implants in herniology

V.P. Zakharov, V.I. Belokonev, I.A. Bratchenko, P.E. Timchenko,
Yu.V. Ponomareva, A.V. Vavilov, L.T. Volova

Abstract. The state of the surface of mesh implants and their encapsulation region in herniology is investigated by laser confocal microscopy. A correlation between the probability of developing relapses and the size and density of implant microdefects is experimentally shown. The applicability limits of differential reverse scattering for monitoring the post-operation state of implant and adjacent tissues are established based on model numerical experiments.

Keywords: laser confocal microscopy, surface microdefects, mesh implant, encapsulation region, hernioplastics, mathematical simulation, Monte Carlo method.

1. Introduction

The purpose of numerous studies with application of various implants (made of polypropylene, polytetrafluoroethylene, carbon fibres) is to find an ideal material, which would provide a combination of high biomechanical characteristics with the efficiency of transplantation and the absence of post-operation aftereffects and relapses [1]. Mesh implants are a kind of endoprotheses, which are produced by spinning artificial fibres of various chemical composition and thickness, using thin single and complex filaments [2]. These implants are about several hundreds of micrometers thick, with the fibre diameter in the range of 50–200 μm . Generally, the most important characteristics determining the choice of a particular implant are the absence of toxicity, compatibility with organism tissues, and the possibility of fast and reliable sterilisation. At the same time, the transplantation efficiency in many practically important cases depends on the response of organism tissues to the implants used, their location among different anatomical structures, stimulation of regeneration, and the change in physico-mechanical properties of transplants during their operation. The comparative estimation of the tissue response to the implantation of synthetic materials

having different physico-chemical properties is of great importance for predicting possible complications.

Note that the processes of incorporation of a transplant depend on its density, resorption time, topology, the presence of surface microdefects (which affect encapsulation of the implant elements), and the formation of vascular and nervous links between tissue layers. The process of transplantation, with allowance for the aforementioned parameters, can be analysed in detail only at the cellular level. Traditionally morphological study of tissues is performed by histological methods using wide-field microscopy [3], as well as by electromyography [4] and ultrasonography [5]. However, all these methods have rather low spatial resolution. To perform a detailed analysis of transplantation, one needs resolution at a level of $\sim 1 \mu\text{m}$ in the tissue layer that obviously contains the implant under study; i.e., one must perform nondestructive three-dimensional analysis and high-resolution monitoring. This requirement can be satisfied using confocal laser microscopy [6], which yields high-contrast images and can differentiate objects with intensities differing by a factor of 200. The purpose of this study was to analyse the specific features of applying confocal laser microscopy in herniology; determine the regularities manifesting themselves with a change in the properties of mesh implants (depending on their shape, type of spinning, and chemical composition) during their intergrowth with organism tissues; and reveal possibilities of detecting different wound pathologies, which arise in the implantation region.

2. Experimental

The confocal laser system was developed based on an inverted Olympus 1X71 optical microscope with a Yokogawa[®] CSU-X1 scanning head, which operates as a Nipkov disk [7]. The laser source was an ALC-400 module with fibre acousto-optic control of radiation of solid-state DPSS lasers with wavelengths of 488 and 532 nm. Images were recorded using an Andor iXON^{EM} EMCCD camera and Andor iQ software. This system made it possible to record up to 2000 optical cuts per second with a transverse and longitudinal resolution of 800 nm.

During the studies we controlled both the microscopic characteristics of implants and the formation of tissues in the presence of an implant, i.e., the implant–tissue interaction.

The materials and properties of the implants under study are listed in Table 1.

V.P. Zakharov, I.A. Bratchenko, P.E. Timchenko S.P. Korolev Samara State Aerospace University, National Research University, Moskovskoe sh. 34, 443086 Samara, Russia;

V.I. Belokonev, Yu.V. Ponomareva, A.V. Vavilov, L.T. Volova Samara State Medical University, ul. Chapaevskaya 89, 443099 Samara, Russia; e-mail: info@samsmu.ru

Received 25 February 2011

Kvantovaya Elektronika 41 (4) 318–323 (2011)

Translated by Yu.P. Sin'kov

Table 1. Main types of mesh implants and their characteristics

Implant type	Composition	Density/g m ⁻²	Porosity (%)	Average defect size/ μm
Prolene Ethicon	Single fibres of isotactic crystalline stereoisomer of polypropylene (115 μm in diameter)	56	60	2–3
Mersilene	Polyethylene terephthalate single fibres (130 μm in diameter)	66	68	15–25
Vipro	Composite prolene–vicryl fibres	93	73	5–40
Esfil light	Polypropylene single fibres (90 μm in diameter, 380 μm thick)	34	92	15–20
Esfil standard	Polypropylene single fibres (120 μm in diameter, 500 μm thick)	62	85	30–40
Esfil heavy	Polypropylene single fibres (140 μm in diameter, 650 μm thick)	95	80	до 60
Unifleks	Polyvinylidene fluoride single filaments (120 μm in diameter, 480 μm thick)	160	85	до 10
Ftoreks	Lavsan complex filaments with a fluoropolymer coating (420 μm in diameter)	48	88	20–25
Optilene [®] Mesh	Polypropylene single fibres (160 μm in diameter)	60	89	40
Optilene [®] Mesh LP	Polypropylene single fibres (140 μm in diameter)	36	89	30
Optilene [®] Mesh Elastic	Polypropylene single fibres (190 μm in diameter)	48	85	40
Premilene [®] Mesh	Polypropylene single fibres (130 μm in diameter)	82	75	15

3. Microscopic analysis of mesh implants

Investigations were performed for two main groups of implants that are widely used in medical practice (Table 1): single-fibre polypropylene meshes and meshes formed of combined fibres, which contain not only synthetic polypropylene filaments but also absorbable sutures (vicryl). The topology and strength of these meshes is determined by the material and fibre diameter, as well as by the spinning type.

Surface microdefects characteristic of different types of mesh implants are shown in Fig. 1. It was found that the surface of Prolene meshes has a smooth structure; however, there are individual, rather large inhomogeneities up to 10 μm in size, which occupy up to 2% of the total mesh surface. Lintex Esfil meshes are characterised by the presence of many small surface defects (the average defect size is in the range of 4–6 μm), whose density increases in the spinning region. Esfil is a single-fibre mesh, composed of two parallel fibres with diameters of 90 (Esfil light), 120 (Esfil standard) and 140 (Esfil heavy) μm ; Esfil light is characterised by surface planar defects with an area of 20 \times 100 μm and a height up to 15 μm , whereas inhomogeneities in Esfil standard have a form of villuses, cones, and spherical inclusions with an average size in the range of 30–40 μm . A similar pattern is characteristic of Esfil heavy but with a larger average size of inhomogeneities (up to 40–60 μm). The area occupied by inhomogeneities is less than 1% of the total surface area for all types of Esfil meshes. However, one must take into account that the fraction of knots in the meshes of this type in the implant volume is fairly large (from 10% to 40%), which makes the implant structure more inhomogeneous.

Single-fibre polypropylene meshes of Optilene[®] Mesh type are characterised by inhomogeneities about 30–40 μm in size, whose fraction is no more than 1% of the total surface area.

The Premilene[®] Mesh implant has the cleanest surface among the polypropylene single-fibre meshes under study. Here, inhomogeneities are rare thornlike protrusions up to 30 μm long and less than 15 μm in diameter; they occupy less than 0.1% surface area.

The implants based on polyethylene terephthalate single fibre (Mersilene mesh) exhibit peeling of individual filaments, which form spike-like defects from 15 to 25 μm in size. Along with these defects, the Mersilene mesh surface contains also individual large inhomogeneities 20–40 μm in diameter, as a result of which the surface area occupied by inhomogeneities increases to 10%–12%.

The implants based on polyvinylidene fluoride single fibres (Unifleks) are characterised by two types of inhomogeneities: small defects about several micrometers in size (which are most likely to be related to the mesh pulling technology, and fairly large inhomogeneities (60–100 μm), comparable with the mesh fibre diameter. The inhomogeneities occupy 5%–7% of the total implant surface.

Complex multifibre mesh implants are generally characterised by a higher degree of inhomogeneity. Here, inhomogeneities of two radically different types can be selected: structural surface defects and spike-like inhomogeneities (loose bundle microfibrils). For example, the Ftoreks implant is a bundle about 100 μm in diameter, composed of Lavsan filaments with fluoropolymer coating \sim 20 μm in diameter. The average size of the spike-like and structural surface inhomogeneities is, respectively, 4–5 and 20–25 μm . The inhomogeneities occupy 2%–3% of the implant surface area.

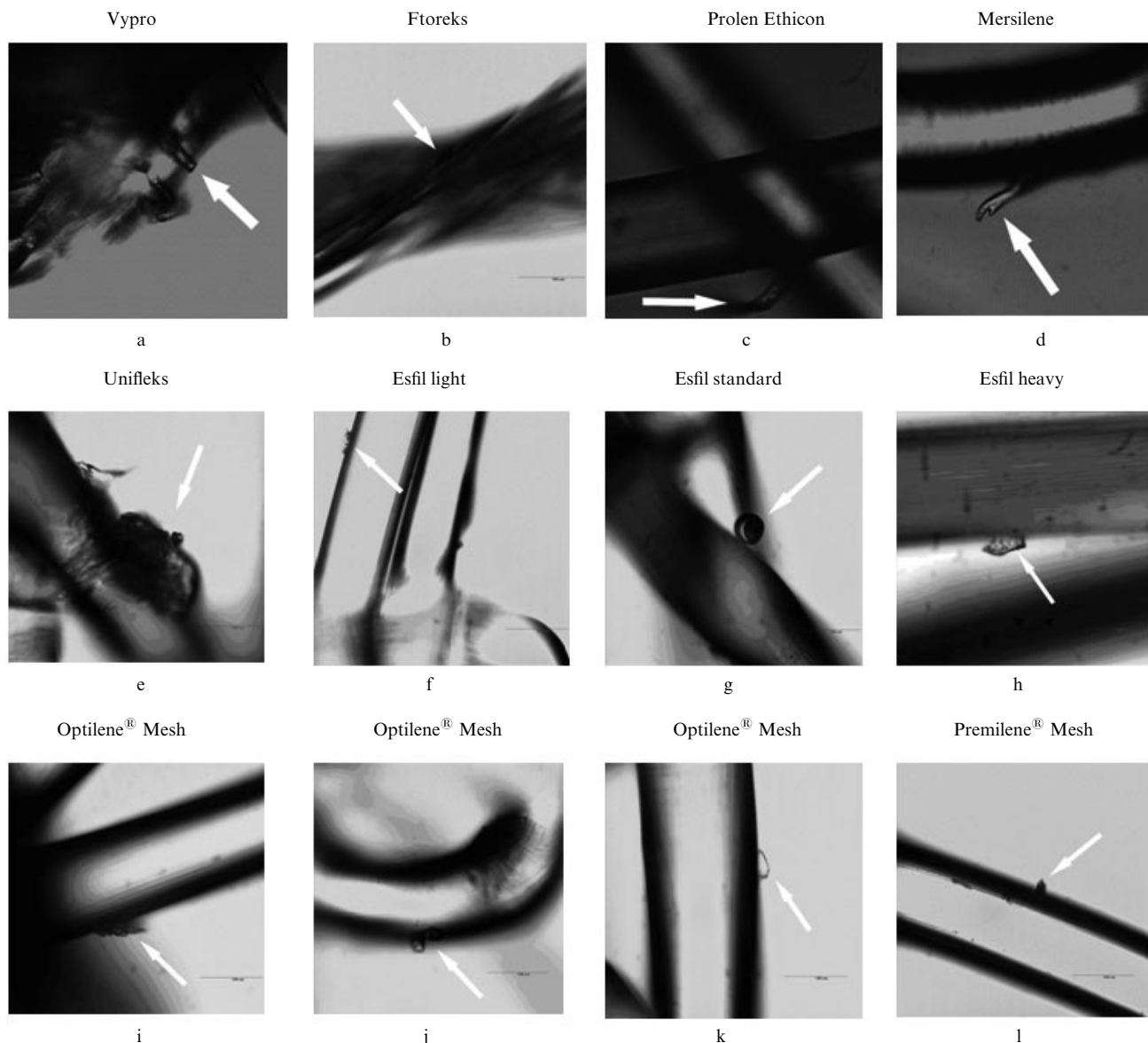


Figure 1. Characteristic surface microdefects for different implants. The image sizes are (a, c, d) $250 \times 250 \mu\text{m}$ and (b, e–l) $400 \times 400 \mu\text{m}$.

The complex mesh Vypro possesses spinning defects, which lead to structural defects of the surface and microscopic violations of its topology. The structure of this mesh is formed by twisting many individual fibres (about $15 \mu\text{m}$ in diameter) into large bundles ($100\text{--}150 \mu\text{m}$ in diameter), due to which many protrusions are observed.

4. Clinical studies of implants

The cytotoxicity and biocompatibility of synthetic implants was estimated on primary cultures of human dermal fibroblasts [8]. Prolene Ethicon, Vypro, and Esfil standard implants were investigated. Each implant ($5 \times 5 \text{ mm}$ in size) was placed in a Petri dish, which contained a previously formed uniform monolayer of cells. Vypro implant caused pronounced alteration and mass death of the cells. The doubling time of cell culture in the growth medium was 27 h, whereas the number of dead cells was larger by a factor of 3.5 than in the check sample. Esfil implant samples, due to their single-filament structure, damaged

only moderately the culture cells. The most pronounced slowing down (by a factor of 1.5 in comparison with the check sample) of the increase in the monolayer density was observed near the surface defects and fibre twist. The damage of the culture cells caused by the Prolene Ethicon implant was the least. In this case, pronounced adhesion of cells to the implant surface (with orientation of fibroblast processes along fibres) was observed.

Experimental studies were performed on 16 white laboratory rats of both sexes, with a mass from 180 to 230 g. Prolene Ethicon or Esfil standard propylene implants were introduced into the abdominal wall of the rats under ether anaesthetic. The check group included four animals. The rats were observed for nine months after the implantation, after which they were killed with ether overdose. The abdominal wall with a polypropylene implant and adjacent tissue was extracted for microscopic studies. The material extracted was fixed in 10% neutral formalin. Commercial cuts were prepared, which were stained with hematoxylin–eosin and with picrofuchsin

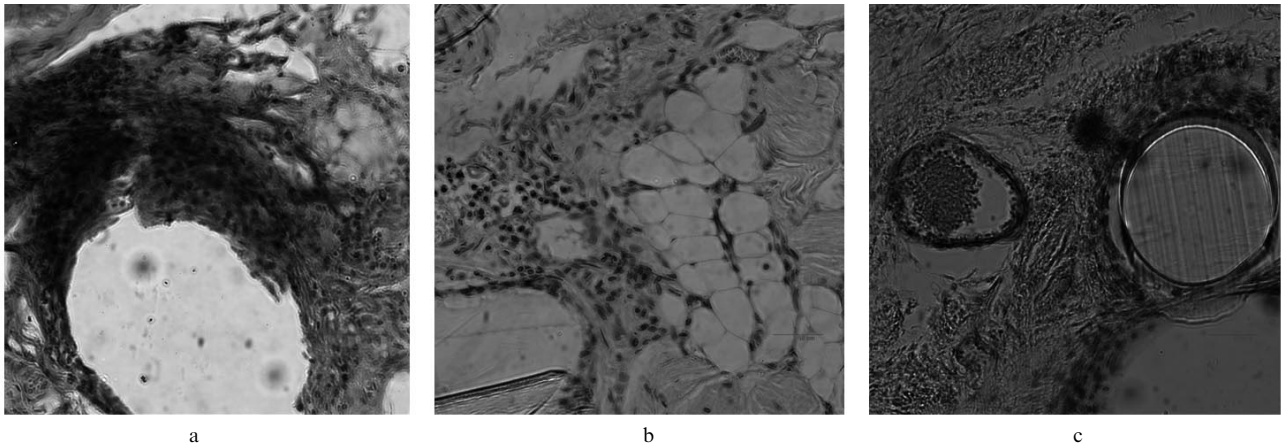


Figure 2. Microscopic photographs ($400 \times 400 \mu\text{m}$) of the pathologies in tissues caused by the presence of a mesh explant: (a) microhaemorrhage, (b) formation of a fat tissue, and (c) backlash.

by the van Gieson's method (Schiff reaction according to McManus). Nine months after the cells of the Esfil implant mesh were surrounded by a thick connecting tissue closely covering the polypropylene filaments. Here, mature collagen fibres are located concentrically, and large rounded cells with large nuclei are in the immediate vicinity of the fibre surface. Individual portions of lymphocytic infiltration are observed, which indicate microhaemorrhages and necrosis development (Fig. 2a).

When using Prolene Ethicon implant, signs of auto-immune process are observed. In particular, the muscular tissue is dropsical, endomysium growth occurs, and some fibres have myocytolysis signs. Macrophages are present near atrophied muscular fibres. The shape of muscular tissues is changed from polygonal to rounded. Nonuniform outgrowth of collagen fibres (immature granulation tissue) around polypropylene filaments is observed in the implant region. There are many fat cells with a cytolemma thinned and a large number of vessels of the microcirculation bed between collagen fibres (Fig. 2b). In fat cells cytoplasm is almost entirely occupied by vacuole. Hyperemia is observed in the microcirculation bed vessels.

Growth of endomysium and fat tissue (which contains many microcirculation bed vessels) is observed in the mesh encapsulation region for implants of both types. Some regions between the connecting tissue and fibres contain voids; they indicate implant backlash, which may lead to a microtrauma in the implantation region (Fig. 2c).

Backlash development at the tissue–fibre implant interface is a threat to integrity of the entire encapsulation region. In the presence of backlash the implant motion in a tissue leads to its mechanical damage, cutting, and development of a microtrauma. The probability of developing a microtrauma increases with an increase in the size, number, and density of microdefects on the implant surface. These defects not only expand the backlash region and hinder implant growing in but also may cause a more significant damage of tissues, such as haemorrhage. Monitoring of mesh implants before the implantation into the organism tissue would make it possible to determine problematic regions, which contain large inhomogeneities and may form backlashes. As a result, the risks of the occurrence of pathological formations in the encapsulation region can be reduced.

Based on the results of clinical studies one can conclude that the spinning homogeneity and the state of implant fibre surface, which are determined by production technology, affect significantly the processes of mesh implant encapsulation. The formation of new tissues near the implant, the rate of wound recovery, the possibility of haemorrhage – all these factors depend directly on the size and density of implant surface inhomogeneities. Near these inhomogeneities the growth of new tissues slows down, the probability of necrotic formation increases, and the presence of large inhomogeneities (comparable in size with the fibre diameter) may lead to mechanical damage of tissue and formation of backlash in the encapsulation region.

5. Estimation of the possibility of optical monitoring of transplantation

The microscopic studies performed show that during the recovery and formation of encapsulation region the main pathological changes in tissues are related to the substitution of normal tissue with fat cells and the formation of a necrotic tissue near the implant fibres. When microhaemorrhage occurs and fat cells arise in the encapsulation region, the tissue loses normal elasticity, which leads to mechanical damage and possible shift of the implant. Timely and precise diagnostics of the development of the above-discussed pathologies in their early stage makes it possible to begin timely treating and reduce the hazard of developing relapses. Note that, in view of the wide wound field, monitoring of the post-operation wound process and detection of possible pathology development can be performed based on the differential analysis of scattered light and detection of inhomogeneities related to the presence of necrotic tissue and/or dystrophic changes in the tissue adjacent to the region occupied by implant fibres.

To estimate the possibilities of monitoring the wound process by the aforementioned method, the mathematical model of multilayer biological medium [9] was extended by adding the encapsulation region with a mesh implant. The distribution of scattered light intensity was determined by the Monte Carlo method [10]; the numerical values of the optical absorption and scattering coefficients were chosen based on the analysis of the experimental data of [11], with subsequent certification in numerical model experiments.

The form, topology, and sizes of mesh implants were chosen based on the samples used in medical practice (Table 1).

Actually, an implant is a distributed scatterer with sharp boundaries, located at a certain depth in a muscular tissue. Hence, the light scattering coefficient of the implant is almost completely determined by the Fresnel coefficients, and the possibility of its detection is determined by the absorption and scattering coefficients of the tissue. The rms calculation error was 6.2%.

As an example, Fig. 3 shows the dependence of the limiting depth, at which the implant mesh can be resolved according to the Rayleigh criterion, on the effective cell size. Curves (1) (scattering and absorption coefficients are 60 and 0.34 mm^{-1}) and (2) (45 and 0.44 mm^{-1} , respectively) specify in fact the visualisation region, which corresponds to the existing spread of absorption and scattering coefficients for a normal muscular tissue. It can be seen that these curves are characterised by two radically different regions. The first is at small mesh cell diameters, where the mesh visualisation depth is mainly related to the image diffusion in light reflected from the implant due to the multiple scattering. The second region corresponds to saturation; it begins with $h \approx 5 \text{ mm}$, when absorption becomes dominant.

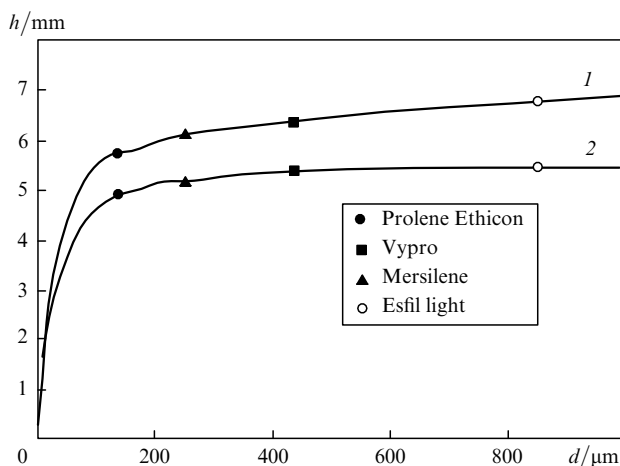


Figure 3. Dependence of the limiting visualisation depth of the mesh implant structure on the effective cell diameter and the characteristics of the medium. The scattering and absorption coefficients are, respectively, (1) 60 and 0.34 mm^{-1} and (2) 45 and 0.44 mm^{-1} .

It can be seen that the visualisation depth for most mesh implants used in practice may exceed 4 mm. However, the most interesting (for practice) is the detection of pathological formations in the implant encapsulation region that give rise to absorption regions in the spectral range of 440–600 nm, nonuniformly distributed along fibres. According to the microscopic studies, encapsulation is significantly affected by the formations whose size is comparable with the fibre diameter. Then, it is convenient to characterise the processes by introducing the effective diameter D of necrotic formation, which is defined as the ratio of the average diameter of necrotic formation to the diameter of mesh implant fibre.

Figure 4 shows the dependence of the minimum effective diameter D for the model of Prolene Ethicon implant on its location depth. One can see that this dependence is linear up to a depth of 1.4 mm (the minimum visible effective

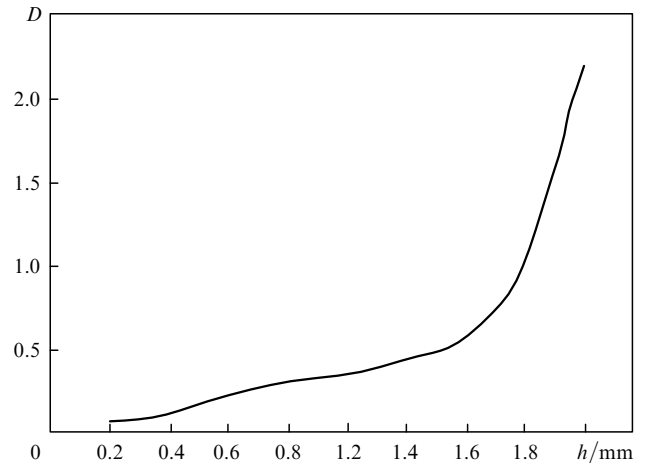


Figure 4. Dependence of the minimum resolved effective diameter of necrotic formations on the implant fibre surface, normalised to the mesh fibre diameter, on the mesh location depth.

diameter of the formation does not exceed the implant fibre diameter), and, beginning with a depth $h \sim 1.5 \text{ mm}$, it becomes highly nonlinear due to the enhanced role of light absorption.

6. Conclusions

It is shown that confocal laser microscopy can be used to analyse the physical state of implants and encapsulation region. It is found that the probability of developing relapses in hernioplastics can be significantly affected by the surface state of mesh implants and their spinning defects; with an increase in size, number, and density of micro-defects, the microtrauma may radically change: a backlash can be formed near the implant surface. To exclude these effects and development of pathologies, it is necessary to perform pre-operational microscopic monitoring of implants. Post-operation monitoring and monitoring of the processes of wound recovery and implant encapsulation can be performed by methods of differential reverse scattering, with visualisation depth as large as 5 mm.

Acknowledgements. This study was supported by the Federal Target Program ‘Scientific and Scientific-Pedagogical Personnel of Innovative Russia’ for 2009–2013.

References

1. Kirpichev A.G., Surkov N.A. *Ispol'zovanie setki iz prolana pri plastike perednei bryushnoi stenki* (Use of Prolan Mesh in the Case of Plastic of the Front Abdominal Wall) (Moscow: Media Sfera, 2001).
2. William S. C., Kent W. K. *Surg. Innovation*, **12**, 63 (2005).
3. Barskii I.Ya., Grammatin A.P., Ivanov A.V. *Opt. Zh.*, **11**, 83 (1999).
4. Vasil'eva-Lipetskaya L.Ya., Rokhanskii A.O., Galatsan A.V., Cherepashchuk G.A., Stepanov A.M., Shabalidas D.A. *Otkrytye informatsionnye i komp'yuternye informatsionnye tekhnologii*, **2**, 215 (1998).
5. Yabe M., Suzuki M., Hiraoka N., Nakada K., Tsuda T. *Radiat. Med.*, **18** (5), 319 (2000).

6. Rajadhyaksha M. *J. Invest. Dermatol.*, **113**, 293 (1999).
7. Egger M.D., Petráň M. *Science*, **157**, 305 (1967).
8. Lefranc S. *Hernia*, **13**, 64 (2009).
9. Zakharov V.P., Bratchenko I.A., Sindyaeva A.R., Timchenko E.V. *Opt. Spektrosk.*, **107**, 957 (2009).
10. Slovetskii S.D. *Radiotekhnika*, **7**, 654 (1994).
11. Tuchin V.V. *Tissue Optics: Light Scattering Methods and Instruments for Medical Diagnosis* (SPIE Tutorial Text in Optical Engineering, 2000).